

# Observing Endocrine Therapy Resistance in Metastatic Breast Cancer with Whole-body MRI

Anwar R. Padhani

Paul Strickland Scanner Centre, Mount Vernon Hospital, Northwood, Middlesex, UK

## Introduction

Approximately 70% of breast cancers are estrogen receptor (ER) positive, and are, therefore, treated with endocrine therapies. However, about 25% of patients with primary disease and almost all patients with metastases will present with or eventually develop endocrine resistance [1]. The mechanisms underlying the development of resistance remain largely unknown but in the last 2 years, several studies have shown ER independent gain-of-function mutations in ESR1, the gene that encodes the ER, in approximately 20–30% of patients with metastatic ER-positive disease who received endocrine therapies, such as tamoxifen and aromatase inhibitors. These mutations lead to ligand-independent ER activity that promotes tumor growth, promoting resistance to endocrine therapy, and potentially enhancing metastatic ability. The emergence of endocrine therapy resistance via this mechanism suggests that, under selective treatment pressure, clonal expansion of rare mutant clones occurs, thus contributing to resistance. Rationale-based novel therapeutic strategies that target these ESR1 mutants have the potential to improve treatment outcomes for patients. Fulvestrant

is a hormonal therapy that specifically targets the ESR1 mutation, that seems to work well in metastatic breast cancer patients with endocrine resistance. Multiple studies suggest greater therapy efficacy in those with bone disease.

In this case study, we demonstrate the potential of quantitative whole-body MR imaging (WB-MRI) to monitor response of breast cancer to hormonal therapy, showing that (1) morphological response does not work as well as diffusion MRI for monitoring response to therapy, (2) that ADC histogram analyses can depict the emergence of treatment resistance, and (3) that spatially discordant response to targeted therapy can emerge when bone disease is effectively treated.

## Patient history

50-year-old woman with metastatic invasive breast cancer, ER positive and HER-2 neu negative disease was initially treated with first line hormonal therapy (Exemestane, Goserelin) and bisphosphonates (Zoledronic acid) for bone only metastatic disease. She was switched to 2<sup>nd</sup> line hormonal therapy with Fulvestrant and Zoledronic on bone disease progression, with good response in her bone disease

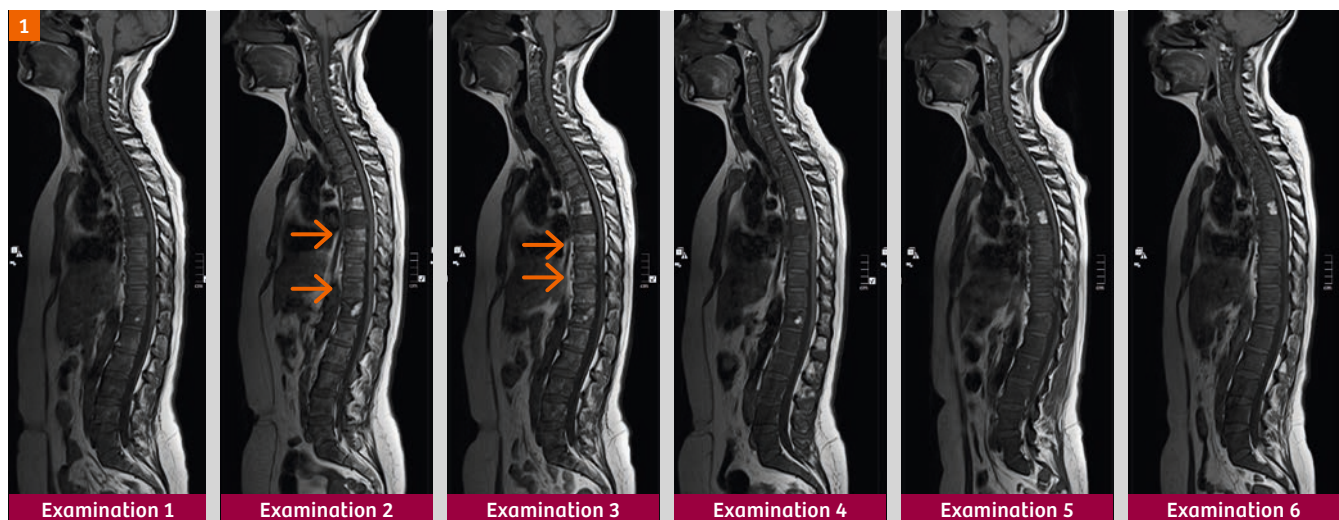


**Figure 1:** Whole-spine T1-weighted images show diffuse bone marrow infiltration with some return of bone marrow fat on examinations 2 and 3 (arrows) with first-line hormonal therapy. The bone marrow fat disappears at therapy relapse on examination 4 and no further T1w changes are detected after therapy change to second-line on examinations 5 and 6. There is a hemangioma in T6.



**Figure 2:** Whole-spine STIR show diffuse bone marrow infiltration with subtle increases in signal intensity with first-line therapy on examinations 2 and 4, but signal intensity lowers by examination 4 at the time of disease relapse (relapse). The bone marrow signal increases again after change to second-line hormonal therapy on examinations 5 and 6. These increases in bone marrow signal intensity are consistent with alternations in tissue water associated with the cell kill mechanism of hormonal treatment (apoptosis).

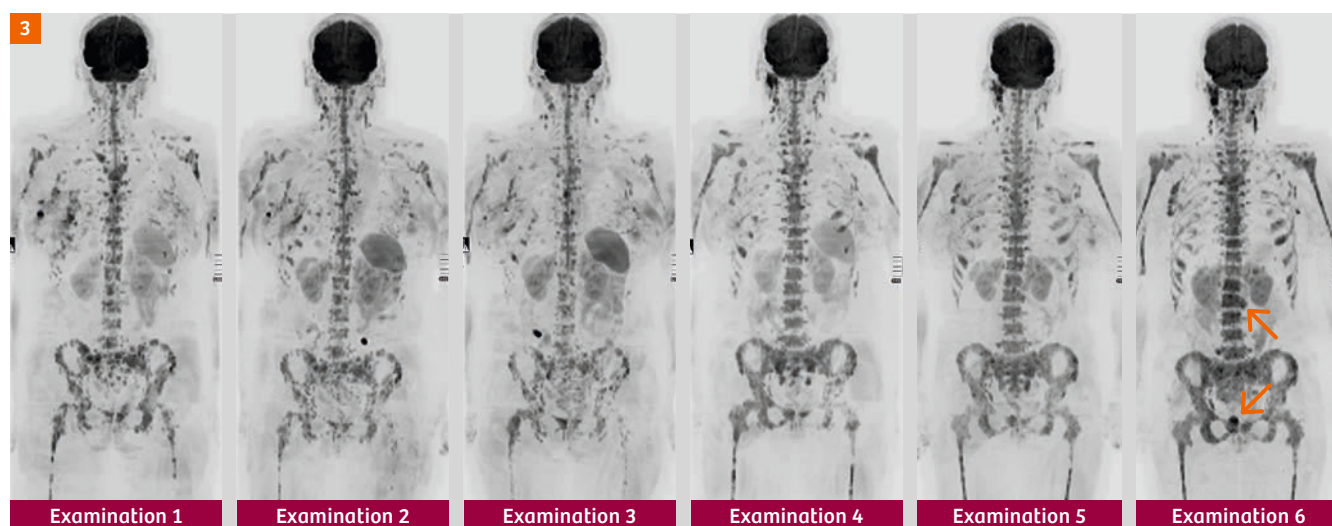


**Figure 3:** Whole-body b900 3D MIP (inverted scale). The bone marrow is diffusely involved with multiple small focal and confluent regions of high-signal intensity in the axial skeleton and in the proximal limb bones. The primary right-sided breast cancer is *in-situ* with axillary nodal disease visible also. Decreases in the signal intensity of bone marrow with first-line therapy can be seen to occur slowly, but there are focal areas of persistent hyperintensities indicating the likely presence of active disease (examination 3). On examination 4, full-blown relapse can be seen, indicated by increases in signal intensity extent in the bones (see article by Padhani & Tunariu on page 64 in this MAGNETOM Flash for progression criteria for bone disease). On changing to second-line hormonal therapy, no response can be confidently identified but there is increasing disease in the anterior ribs, on the left side of L2 and pubic symphysis (arrows).

only shown on quantitative diffusion imaging. Unfortunately, she also developed liver and pancreas metastases needing further therapy change to chemotherapy. No regional radiotherapy has been administered.

Serial examinations with whole-body diffusion MRI were undertaken using published protocols [2]. Whole-body diffusion sequences using b-values of b50, b600 and

900 s/mm<sup>2</sup> were undertaken together with spinal T1-weighted and STIR sequences, to monitor response to treatment. Six examinations were performed in total. Following the baseline examination, three further examinations were done while on first-line hormonal therapy and two examinations while on second-line hormonal therapy.



**Figure 4:** WB-tumor load segmentations were undertaken on syngo.via Frontier MR Total Tumor Load software (Siemens Healthcare, Erlangen, Germany; released research prototype). The whole-body b900 images are segmented using computed high b-value images of 1000–1200 s/mm<sup>2</sup>, setting a signal intensity threshold of approximately 100 AU. Extraneous signals (such as the brain, kidneys and bowel) are removed, to leave only recognizable bone disease sites including the right breast and axilla. The color the b900 MIP images are overlaid with ADC value classes using the following thresholds. The green voxels are values  $\geq 1500 \mu\text{m}^2/\text{s}$  (representing voxels that are ‘highly likely’ to be responding). The yellow voxels are set to lie between the 95<sup>th</sup> centile ADC value of the pre-treatment (examination 1 or examination 4) histograms (1256 and 1127  $\mu\text{m}^2/\text{s}$  respectively) and 1500  $\mu\text{m}^2/\text{s}$ . Thus, yellow voxels represent regions ‘likely’ to be responding. Red voxels represent mostly areas that are untreated disease or have no detected response.

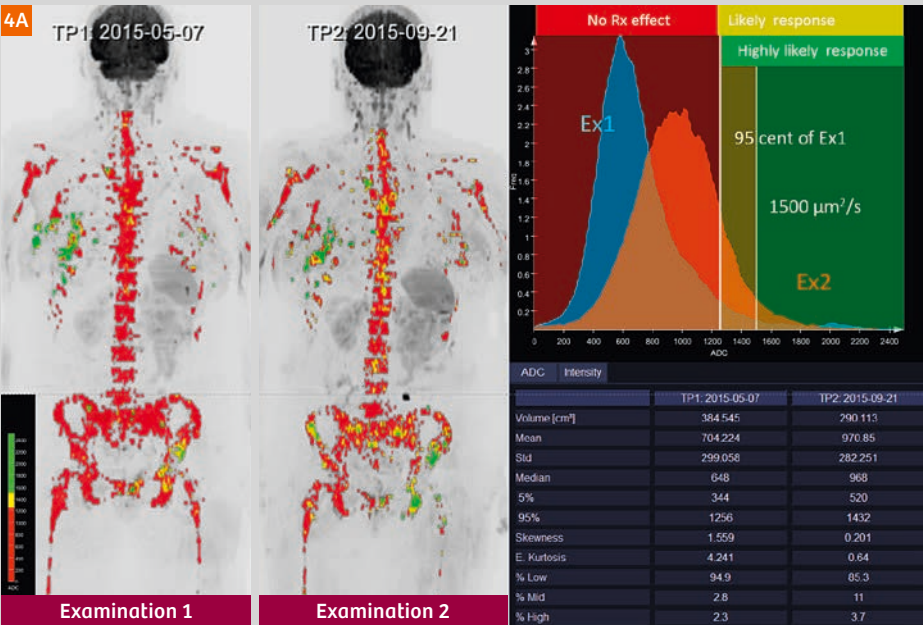


**Figure 4A: Histogram analysis of examination 1 and 2.** 384 ml of tumor was segmented before therapy and 290 ml on therapy. Note that there is a significant global increase in ADC values (704  $\mu\text{m}^2/\text{s}$  and 971  $\mu\text{m}^2/\text{s}$ ) and a decrease in kurtosis (4.2 and 0.6) on the corresponding relative frequency histograms indicating some response on a whole-body basis. Note increasing numbers of yellow and green voxels occurring in patches (for example the left hip – note no radiotherapy has been given). These appearances taken with morphologic assessments indicate a favourable response overall with no evidence of progression.

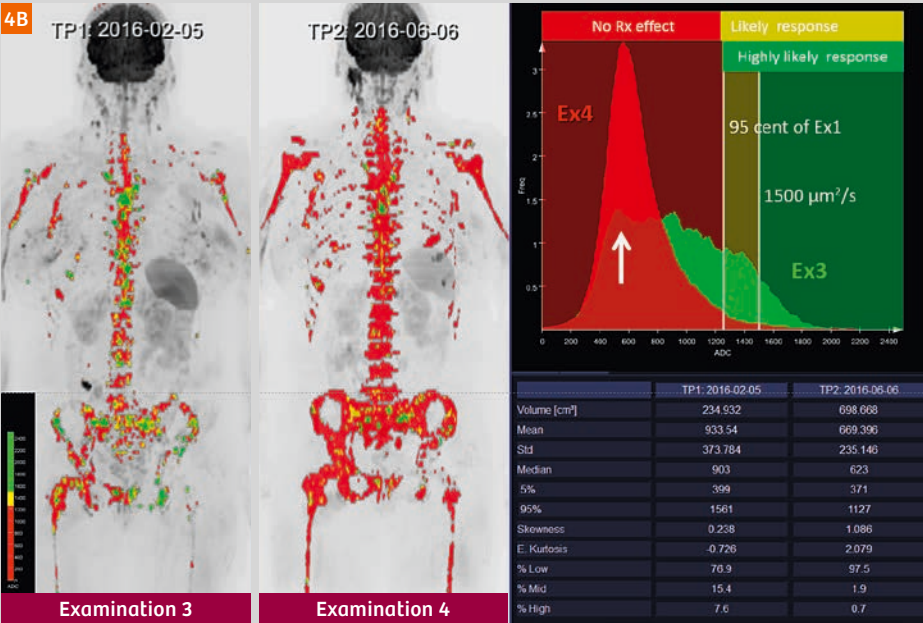


**Figure 4B: Histogram analysis of examination 3 and 4.** 235 ml of tumor was segmented on examination 3 and 698 ml on examination 4 at disease relapse. Note that on examination 3 there is a flattened histogram (green histogram) with a significant global increase in ADC values (933  $\mu\text{m}^2/\text{s}$ ) compared to baseline and a marked decreased kurtosis (-0.7) on the relative frequency histograms, indicating a good response to first-line hormonal therapy. Note increasing numbers of yellow and green voxels. These appearances taken with morphologic assessments indicate a good response overall. However, note persistent red voxels on examination 3 and a corresponding peak on the examination 3 histogram, indicating areas of therapy resistance (vertical white arrow). On examination 4, the patient has relapsed with a histogram that is identical to the baseline pretherapy study (examination 1).



**Figure 4C: Histogram analysis of examination 5 and 6.**

617 ml of tumor was segmented on examination 5 and 883 ml on examination 6. Note that on both examinations, the histograms show significant global increases in ADC values (956 and 904  $\mu\text{m}^2/\text{s}$ ) compared to examination 4 (pre-second-line treatment baseline) indicating a good response to second-line hormonal therapy. The diffusion imaging appearances indicate a good response overall not observable on the T1w spine images. However, note that there are persistent red voxels on both examinations 5 and 6, indicating persistent areas of therapy resistance in the bones. Note also increased volume of right axillary nodal disease. Therapy was changed because of new liver and pancreatic metastases.

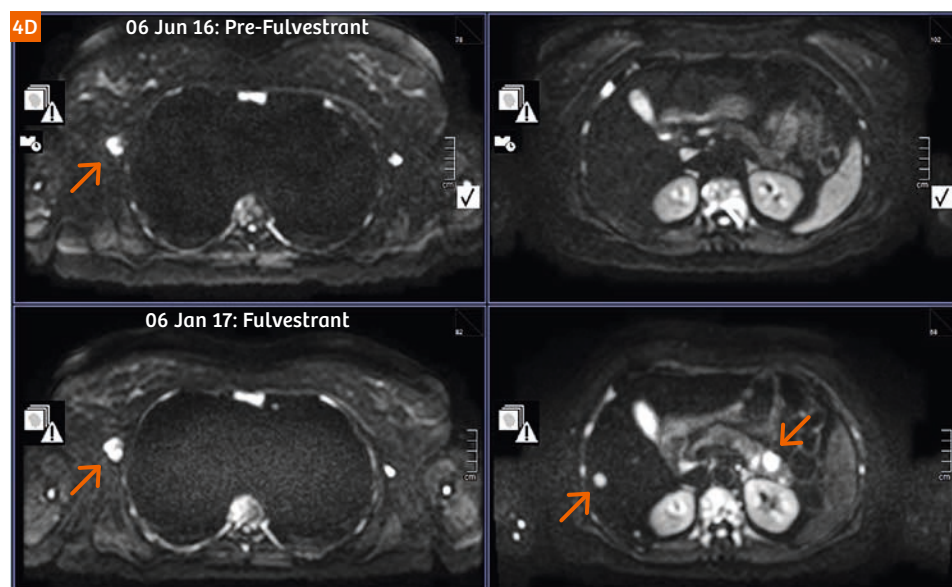


**Figure 4D: Axial b900 images of the upper abdomen for examinations 4 (pre-second-line hormonal therapy) and 6 show the emergence of new disease in liver and pancreas (arrows), resulting in a change to chemotherapy therapy. Right axillary nodes are also enlarging.**

## References

- 1 Jeselsohn R, Buchwalter G, De Angelis C, Brown M, Schiff R. ESR1 mutations – a mechanism for acquired endocrine resistance in breast cancer. *Nat Rev Clin Oncol*. 2015;12:573–583.
- 2 Padhani AR, Lecouvet FE, Tunariu N, et al. METastasis Reporting and Data System for Prostate Cancer : Practical Guidelines for Acquisition , Interpretation , and Reporting of Whole-body Magnetic Resonance Imaging-based Evaluations of Multiorgan Involvement in Advanced Prostate Cancer. *Eur Urol*. European Association of Urology; 2017;71:81–92.

## Contact



Professor Anwar R. Padhani  
MB, BS, FRCP, FRCR  
Paul Strickland Scanner Centre  
Mount Vernon Hospital

Rickmansworth Road  
Northwood, Middlesex HA6 2RN  
United Kingdom  
anwar.padhani@  
stricklandscanner.org.uk